Theoretical study for the excited states of $MoO_{4-n}S_n^{2-}$ ($n=0\sim4$) and $MoSe_4^{2-}$

Hiroshi Nakatsuji[a] and Shinji Saito
Division of Molecular Engineering, Graduate School of Engineering, Kyoto University, Kyoto 606, Japan

(Received 13 March 1990; accepted 24 April 1990)

Ground and excited states of six molybdenum complexes, $MoO_{4-n}S_n^{2-}$ ($n=0\sim4$) and $MoSe_4^{2-}$, are systematically studied by symmetry adapted cluster (SAC) and SAC-CI theories. In the ground states, the ionicity of MoO_4^{2-} is much larger than those of MoS_4^{2-} and $MoSe_4^{2-}$. The calculated electronic spectra compare well with the observed spectra. New systematic assignments of the spectra are given. Most of the peaks are assigned to the electron-transfer type transitions from ligands to the metal. Many assignments are different from the previous ones. The observed relationships in the electronic spectra of these complexes are examined and corrected. The solvation effect is argued briefly.

PACS numbers:

I. INTRODUCTION

Transition metal complexes have a variety of excited states in a relatively lower energy region, owing to an existence of filled and unfilled *d*, *s*, and *p* orbitals in a relatively narrow energy region. The ligand–metal interaction and the metal–metal interaction also cause a variety of excited states. Therefore, reliable theoretical studies on excited states are very important for assignments of observed spectra and for understanding natures of excited states. However, reliable *ab initio* calculations are very few even for simple complexes. This is probably due to the fact that large scale calculations are necessary even for small-size complexes.

We have recently studied the excited and ionized states of RuO_4 and OsO_4.[1] Their electronic spectra were observed up to just below the first ionization energy.[2] We have assigned whole regions of the spectra and shown the natures of the transitions. For the ionized states, the breakdown of a one particle model is noted even in a relatively lower energy region.

A systematic measurement of the electronic spectra is reported[3–8] for the molybdenum complexes, $MoO_{4-n}S_n^{2-}$ ($n=0\sim4$) and $MoSe_4^{2-}$. Magnetic circular dichroism spectra are also measured for these complexes.[9] From these spectra, the following relationships are pointed out:[5]

$$\nu_1(MoO_3S^{2-}) \approx \nu_1(MoO_2S_2^{2-}) \approx \nu_2(MoOS_3^{2-}), \quad (1)$$

$$\nu_2(MoO_3S^{2-}) \approx \nu_3(MoO_2S_2^{2-}), \quad (2)$$

$$\nu_2(MoO_2S_2^{2-}) \approx \nu_3(MoOS_3^{2-}) \approx \nu_2(MoS_4^{2-}), \quad (3)$$

$$\nu_1(MoOS_3^{2-}) \approx \nu_1(MoS_4^{2-}), \quad (4)$$

where $\nu_i(C)$ is the wavelength of the i-th band maximum in the observed electronic spectrum of the complex C. Experimentally, it is known that $MoO_{4-n}S_n^{2-}$ ($n=1\sim4$) are synthesized successively when hydrogen sulphide gas is passed into an aqueous solution of MoO_4^{2-}.[10] The semiempirical SCCC-MO calculations,[11,12] the $X\alpha$ methods,[13–15] and the local density method[16] were reported for these complexes, but no theoretical studies have yet tested quantitatively the above relationships.

In this paper, we systematically study the excited states of the complexes $MoO_{4-n}S_n^{2-}$ ($n=0\sim4$) and $MoSe_4^{2-}$ by using the symmetry adapted cluster (SAC) expansion theory for the ground state and the SAC-CI theory for the excited states. We theoretically examine the validity of the above relationships. Furthermore, there are complete measurements of the ^{95}Mo chemical shifts of these complexes,[17] and we have successfully studied them by an *ab initio* theory.[18] In particular, we have calculated magnetically allowed *d–d* transition energies of these complexes by the present method and used them for clarifying the mechanism of the ^{95}Mo chemical shifts of these complexes.[19]

II. COMPUTATIONAL DETAILS

The structures of the complexes are summarized in Table I. They are the experimental values[20–24] except for MoO_3S^{2-}, for which the geomery is estimated by interpolation.

The basis sets used in this study are as follows. The relativistic effective core potential (ECP)[25] and the (3*s*3*p*4*d*)/[3*s*2*p*3*d*] set[25] are employed for Mo atom. The (9*s*5*p*)/[3*s*2*p*] set[26] is used for oxygen and the ECP[27] and the (3*s*3*p*)/[2*s*2*p*] set[27] for sulphur and selenium. The Hartree–Fock (HF) orbitals are claculated by the program GAMESS.[28]

The electron correlations in the ground states of the complexes are calculated by the SAC theory[29] and those in the excited states by the SAC-CI theory[30] with the use of the program SAC85.[31] The active orbitals consist of 43 HF orbitals, 12 higher occupied orbitals and 31 lower unoccupied orbitals. The number of the linked operators is reduced by the configuration selection procedure.[32] All single-excitation operators are included without doing selection. For double-excitation operators, we use the threshold $\lambda_g = 3\times10^{-5}$ hartree for the ground state and $\lambda_e = 1\times10^{-4}$ hartree for the excited states.[32] The triple and quadrupole excitations are considered in the unlinked terms. They are

[a] All correspondences should be addressed to the present address which is the Department of Synthetic Chemistry, Faculty of Engineering, Kyoto University, Kyoto, Japan.

 0021-9606/90/151865-11$03.00

TABLE I. Structures of $MoO_{4-n}S_n^{2-}$ ($n = 0 \sim 4$) and $MoSe_4^{2-}$.[a]

	MoO_4^{2-}[b]	MoO_3S^{2-}[c]	$MoO_2S_2^{2-}$[d]	$MoOS_3^{2-}$[e]	$MoOS_3^{2-}$[f]	$MoSe_4^{2-}$[g]
Symmetry	T_d	C_{3v}	C_{2v}	C_{3v}	T_d	T_d
Mo–O	1.765	1.77	1.758	1.785		
Mo–S		2.19	2.188	2.178	2.18	
Mo–Se						2.31
<OMoO	109.47	109.47	112.62			
<OMoS		109.47		110.5		
<SMoS			107.68	109	109.47	
<SeMoSe						109.47

[a] Distances are in Å and angles in degree.
[b] Reference 20.
[c] Estimated values.
[d] Reference 21.
[e] Reference 22.
[f] Reference 23.
[g] Reference 24.

expressed as the products of the single- and double-excitation operators which are important in the preliminary CI for the states under consideration. Owing to the merits of the SAC and SAC-CI theories, the dimensions are small in comparison with those of an ordinary CI of comparable accuracy.

III. RESULTS AND DISCUSSION

A. Ground state

Figure 1 shows the orbital energy levels of all the molecular orbitals (MOs) included in the active spaces. The HF

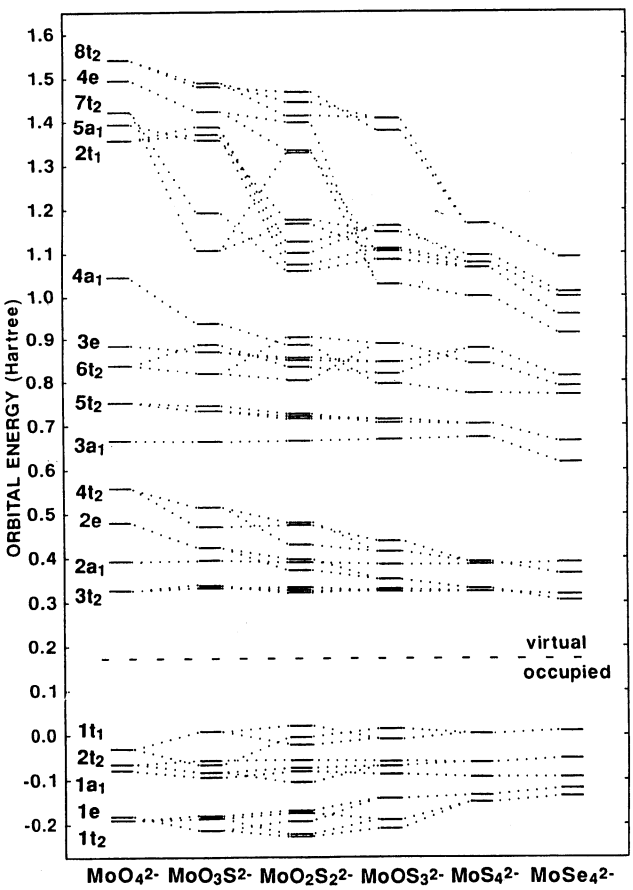

FIG. 1. Orbital energy levels of the active spaces for $MoO_{4-n}S_n^{2-}$ and $MoSe_4^{2-}$.

configuration of the ground state of MoO_4^{2-} is written as

$$(1t_2)^6(1e)^4(1a_1)^2(2t_2)^6(1t_1)^6\ (3t_2)^0(2a_1)^0(2e)^0(4t_2)^0.$$

The characters of these MOs are as follows:

$1t_2$: σ bonding between M(d) and O(p), M(d_σ) + O(p_σ),
$1e$: π bonding between M(d) and O(p), M(d_π) + O(p_π),
$1a_1$: nonbonding O(p),
$2t_2$: weakly bonding O(p),
$1t_1$: weakly antibonding O(p),
$3t_2$: nonbonding M(p),
$2a_1$: nonbonding M(s),
$2e$: π antibonding between M(d) and O(p), M(d_π) − O(p_π),
$4t_2$: σ antibonding between M(d) and O(p), M(d_σ) − O(p_σ),

where M(d) and O(p) denote valence d and p orbitals on metal and oxygen, respectively, and plus and minus signs indicate bonding and antibonding combinations, respectively. When the oxygen ligand is substituted by S or Se, the coefficient of M(s) in the $1a_1$ MO increases and those of M(p) and L(p) in the $4t_2$ MO increase.

There are two general changes in the occupied MOs as the ligand is substituted. Since the $2t_2$ and $1t_1$ MOs (or those correlated to them in the lower symmetries) are principally ligand orbitals, their orbital energies change as the ligand is substituted. The energies of the $1e$ and $1t_2$ MOs increase when the oxygen ligand is substituted by S and further by Se. The changes of the virtual MOs are more remarkable than those of the occupied MOs. In particular, those of the $2e$ and $4t_2$ MOs are remarkable. The levels of the $3t_2$ and $2a_1$ MOs are constant, since they mainly consist of the metal AOs. Jostes *et al.*,[12] however, considered in their SCCC-MO calculations that the energy levels of the virtual MOs do not change much and therefore the differences in the observed spectra are chiefly attributed to the changes of the occupied MOs. Table II gives the experimental force constants for the stretching of the M–L bonds,[22,23] and indicates that the M–L bond becomes stronger as the hardness of the ligand increases.

Figure 2 shows net atomic charges on M and L calculat-

TABLE II. Experimental stretching force constants of $MoO_{4-n}S_n^{2-}$ ($n = 0 \sim 4$) and $MoSe_4^{2-}$ (mdyn/Å).

	MoO_4^{2-} [a]	MoO_3S^{2-} [b]	$MoO_2S_2^{2-}$ [b]	$MoOS_3^{2-}$ [a]	MoS_4^{2-} [a]	$MoSe_4^{2-}$ [b]
Mo–O	5.85	5.83	5.87	5.89		
Mo–S		3.12	2.93	3.10	3.18	
Mo–Se						2.62

[a] Reference 22.
[b] Reference 33.

ed by the HF and SAC methods for the ground state of each complex. The electron distributions obtained by the HF method are more ionic than those by the SAC method, since the HF method overestimates ionic configurations. By the inclusion of electron correlations, 0.2 ~ 0.4 electron is redistributed. This tendency was also seen previously for RuO_4 and OsO_4.[1] The differences in the Mo net charge among MoO_4^{2-}, MoS_4^{2-}, and $MoSe_4^{2-}$ are particularly interesting. Although the difference between MoS_4^{2-} (-0.200) and $MoSe_4^{2-}$ (-0.259) is small, that between MoO_4^{2-} ($+1.294$) and MoS_4^{2-} (-0.200) is as large as 1.49 and even the sign is inverted. The Pauling's electronegativities[34] of the O, S, Se, and Mo atoms are 3.5, 2.5, 2.4, and 1.8, respectively.

Table III shows the AO Mulliken population analyses obtained by the SAC calculation. We note that the population analyses should be considered as showing only a qualitative tendency, as the population in the Mo 5*s* orbital of MoO_4^{2-} is negative in sign! As a number of the soft ligands increases, the population of the ligand *p* AO gradually decreases and those of the metal *s*, *p*, and *d* AOs increase. These differences show that the electron distribution and the nature of the M–L bond of MoO_4^{2-} are different from those of MoS_4^{2-} and $MoSe_4^{2-}$.

Furthermore, it is expected that in a polar solvent the solvation effect for MoO_4^{2-} should considerably differ from those for MoS_4^{2-} and $MoSe_4^{2-}$, though a large difference is not expected between MoS_4^{2-} and $MoSe_4^{2-}$. In the ground state, the solvation energy of MoO_4^{2-} should be larger than those of MoS_4^{2-} and $MoSe_4^{2-}$. In Fig. 3, we illustrate the expected difference in the solvation energy: MoO_4^{2-} would belong to type I and MoS_4^{2-} and $MoSe_4^{2-}$ to type II. More details of this figure will be explained later.

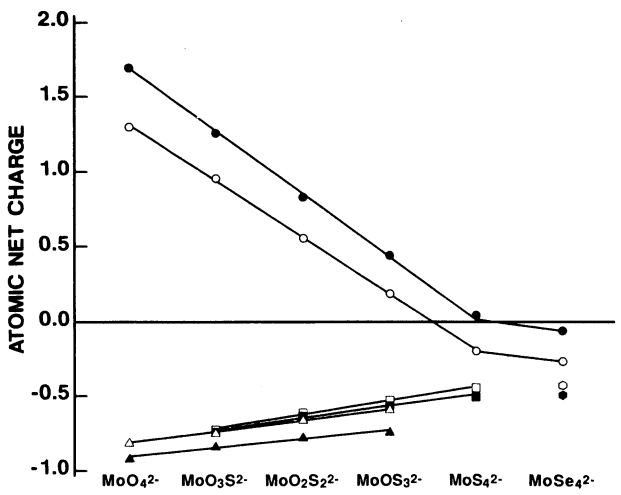

FIG. 2. Atomic net charges of M and L in $MoO_{4-n}S_n^{2-}$ and $MoSe_4^{2-}$ by the HF and SAC methods. ● and ○ are the atomic charges on Mo, ▲ and △ are on O, ■ and □ are on S, and ● and ○ on Se by the HF and SAC methods, respectively.

B. Excited states

Tables IV–IX give the experimental and theoretical excitation energies and oscillator strengths for $MoO_{4-n}S_n^{2-}$ ($n = 0 \sim 4$) and $MoSe_4^{2-}$. Figures 4, 5, 7–10 show the comparison between experimental and theoretical spectra: the upper one the experimental spectrum and the lower one the theoretical spectrum.

1. MoO_4^{2-}

The excitation energies and oscillator strengths obtained by experiments[3,4] and by the present and previous calculations[11,13–15] are summarized in Table IV. The experimental spectrum shown in Fig. 4 was measured in a single crystal of Cs_2SO_4 at the low temperature.[3] The spectrum observed for an aqueous solution of $Na_2MoO_4 \cdot 2H_2O$ (Ref. 4) is shown in the inset of Fig. 4. The lowest peak is observed at 5.30 ~ 5.69 eV (Ref. 3) and at 5.36 eV.[4] In the T_d symmetry, only the transitions to the T_2 states are dipole allowed. The first allowed transition calculated by the present theory is to the $1T_2$ state $[1t_1\,(O(p)) \rightarrow 3t_2(M(d))]$ lying at 4.37 eV above the ground state, but the oscillator strength is very small. No peaks are observed at this range of the experimental spectrum as expected. The transition to the $2T_2$ state calculated at 5.14 eV has a considerable amount of oscillator strength. This is the transition from the $2t_2$ ($O(p)$) MO to the $3t_2$ ($M(d)$) MO. We assign this transition to the lowest observed peak. However, the previous experiments[3,4] and calculations[11–13,35] have assigned this peak to the transition from the $1t_1$ MO to the $2e$ MO. In those papers,[3,4,11–15,35] the MO ordering near the HOMO and LUMO was

$$2t_2 < 1t_1 < 2e < 3t_2, \tag{5}$$

and the characters of the $2e$ and $3t_2$ MOs were the localized $M(d)$ orbital and the antibonding orbital between $M(d)$ and $O(p)$, respectively. Their ordering and characters are different from the present ones shown in Fig. 1 as noted in Sec. III A.

The third and fourth allowed states are $3T_2[1t_1(O(p)) \rightarrow 2e(M(d) - O(p))]$ and $4T_2[1a_1(O(p)) \rightarrow 3t_2(M(d))]$ calculated at 5.52 and 5.67 eV above the ground state. In the solution spectrum shown in the inset of Fig. 4, there are no

TABLE III. Atomic orbital Mulliken population of $MoO_{4-n}S_n^{2-}$ ($n = 0 \sim 4$) and $MoSe_4^{2-}$ calculated by the SAC method.

	Mo			O			S		Se	
	5s	5p	4d	1s	2s	2p	3s	3p	4s	4p
MoO_4^{2-}	−0.204	0.581	4.329	1.999	1.917	4.907				
MoO_3S^{2-}	0.018	0.674	4.354	1.999	1.918	4.828	1.808	4.913		
$MoO_2S_2^{2-}$	0.160	0.798	4.489	1.999	1.917	4.745	1.816	4.799		
$MoOS_3^{2-}$	0.249	0.907	4.654	1.999	1.923	4.675	1.824	4.708		
MoS_4^{2-}	0.319	1.036	4.845				1.828	4.622		
$MoSe_4^{2-}$	0.465	0.934	4.860						1.831	4.604

peaks except for the two at 5.36 and 5.95 eV. However, in the single crystal spectrum, some peaks whose progressions are different from neither the first one nor the second one are measured.[3] They are considered as being due to different electronic states or to an overlap effect. We consider this peak system to be assigned to the $3T_2$ and $4T_2$ states from the calculated energy and oscillator strength. These transitions correspond to the electron transfer from O to M.

The second band maximum is observed at 5.87∼6.48 eV (Ref. 3) and at 5.95 eV.[4] We assign this band to the transition to the $5T_2$ state $[2t_2(O(p)) \rightarrow 2a_1(M(s))]$, though all the previous assignments, both experimental and theoretical, were $2t_2 \rightarrow 2e$.[4,12–15] This is an electron transferred excitation from O to M.

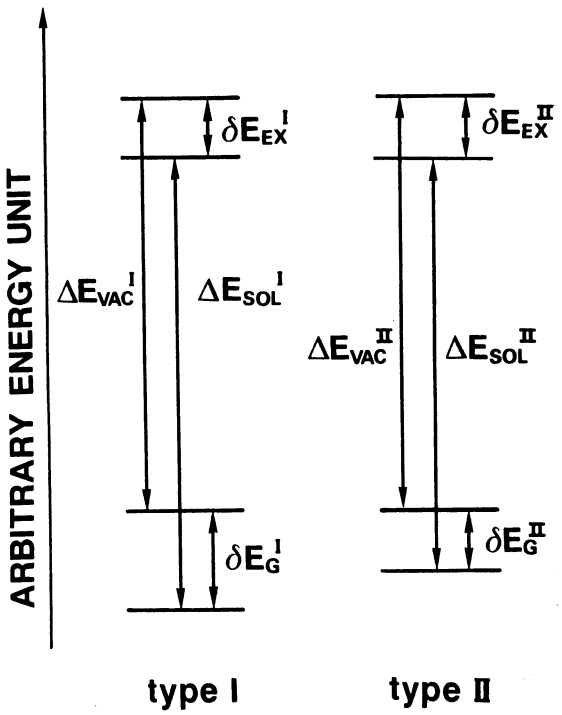

FIG. 3. Polar solvent effects on the energy levels of the ground and excited states. δE_G and δE_{EX} show the stabilization energies for the ground and excited states, respectively, due to the polar solvent effect. ΔE_{VAC} and ΔE_{SOL} denote the excitation energies in vacuum and in a solution, respectively. Following relations exist between δE_G and δE_{EX}; namely $\delta E_G^I > \delta E_{EX}^I$ in type I, $\delta E_G^{II} \approx \delta E_{EX}^{II}$ in type II, and $\delta E_G^I > \delta E_G^{II}$.

Müller *et al.* considered experimentally that the next band exists in the region larger than 6.82 eV.[4] As a candidate for this band the present study indicates the next allowed peak $[2t_2(O(p)) \rightarrow 2e(M(d) - O(p))]$ calculated at 6.52 eV.

Though our assignments of the spectra of MoO_4^{2-} are different from those reported previously,[10–15] the excitation energies and the oscillator strengths obtained by the present calculation agree well with the experimental values.[3,4] The average discrepancy between the experimental and theoretical excitation energies is 0.21 eV.

Since the ionicity of the M–O bond is reduced in these excited states of MoO_4^{2-}, we expect that the solvation energy in a polar solvent should decrease after excitation. Then, it is anticipated that the excitation energies in a polar solvent would be larger than those in vacuum, as shown in type I diagram of Fig. 3.

The present results give the crystal splitting parameter, Δ value, as 1.15 eV, in comparison with the results of the $X\alpha$ methods, 2.05 eV (Ref. 14) and 1.8 eV (Ref. 15).

2. MoO_3S^{2-}

Table V gives the experimental[5] and theoretical excitation energies and oscillator strengths for MoO_3S^{2-}. The experimental spectrum shown in Fig. 5 were observed in an aqueous solution.[6] The symmetry of the molecule reduces to C_{3v} so that the triply degenerate MOs split into doubly degenerate and nondegenerate MOs. The overall ordering of the MOs is the same as that of MoO_4^{2-}. The lowest virtual MO, 5e, is derived from the $3t_2$ MO and does not correspond to the 2e MO of MoO_4^{2-}.

In the present calculation, there are no excited states below 4.08 eV, though a peak is observed at 3.15 eV in the experimental spectra.[5,6] The solvation effect does not explain this difference because the excitation energy in a gas phase should be smaller than that in a polar solvent. MoO_3S^{2-} is rather difficult to isolate[36] because in the following reactions,

$$MoO_4^{2-} \xrightarrow[\text{(i)}]{H_2S} MoO_3S^{2-} \xrightarrow[\text{(ii)}]{H_2S} MoO_2S_2^{2-} \xrightarrow[\text{(iii)}]{H_2S} MoOS_3^{2-} \xrightarrow[\text{(iv)}]{H_2S} MoS_4^{2-}, \quad (6)$$

step (ii) is very fast and MoO_3S^{2-} is a kinetically labile species. Figure 6 shows the experimental spectra of MoO_3S^{2-} (Ref.6) and $MoO_2S_2^{2-}$,[6] and, in addition, the scaled

TABLE IV. Excitation energies of MoO_4^{2-} in eV.

Experimental			Theoretical						
	Ref. 4		SAC-CI						
Ref. 3	ΔE	f[c]	ΔE	f[c]	Main configuration[f]	SCCC[a]	Xα[b]	Xα[c]	Xα[d]
			4.37	4.5(−4)[g]	$1T_2(1t_1\rightarrow 3t_2)$				
			4.43		$1E(1t_1\rightarrow 3t_2)$				
			4.44		$1T_1(1t_1\rightarrow 3t_2)$				
			4.60		$1A_2(1t_1\rightarrow 3t_2)$				
			4.94		$2T_1(2t_2\rightarrow 3t_2)$				
			5.11		$3T_1(1t_1\rightarrow 2e)$				
			5.13		$1A_1(2t_2\rightarrow 3t_2)$				
5.30 – 5.69	5.36	0.06	5.14	0.049	$2T_2(2t_2\rightarrow 3t_2)$	5.94[h]	5.17[h]	4.48[h]	5.5[h]
			5.20		$2E(2t_2\rightarrow 3t_2)$				
			5.48		$4T_1(2t_2\rightarrow 2a_1,2t_2\rightarrow 3t_2)$				
5.77–			5.52	0.026	$3T_2(1t_1\rightarrow 2e)$				
5.79[i]			5.67	0.014	$4T_2(1a_1\rightarrow 3t_2)$				
			5.81		$5T_1(2t_2\rightarrow 2a_1)$				
5.87 – 6.48	5.95	0.2	6.06	0.081	$5T_2(2t_2\rightarrow 2a_1)$		5.84[j]	4.60[j]	5.6[j]
			6.45		$3E(1a_1\rightarrow 2e)$				
	>6.82[k]		6.52	0.118	$6T_2(2t_2\rightarrow 2e)$			6.53[l]	7.3[l]
			6.56		$2A_1(1a_1\rightarrow 2a_1)$				

Average discrepancy 0.21

[a] Reference 11.
[b] Reference 13.
[c] Reference 14.
[d] Reference 15.
[e] Oscillator strength.
[f] Indicated relative to the HF configuration $(1t_2)^6(1e)^4(1a_1)^2(2t_2)^6(1t_1)^6$.
[g] Characteristic base 10 given in parenthesis.
[h] Transition is $1t_1\rightarrow 2e$.
[i] See the text.
[j] Transition is $3t_2\rightarrow 2e$.
[k] Estimated value.
[l] Transition is $1t_1\rightarrow 4t_2$.

$MoO_2S_2^{2-}$ spectrum whose absorption coefficient of the first band is set equal to that of MoO_3S^{2-}. The higher bands than the first one of the scaled $MoO_2S_2^{2-}$ spectrum are hidden under the spectrum of MoO_3S^{2-}. We thus conclude that the peak observed at 3.15 eV is not due to MoO_3S^{2-} itself but due to the complex, $MoO_2S_2^{2-}$. This conclusion is also supported by our study of ^{95}Mo–NMR chemical shift for the series of the complexes $MoO_{4-n}S_n^{2-}$ $(n=0\sim 4)$ and $MoSe_4^{2-}$.[19] Thus, the first equality of Eq. (1) proposed experimentally is wrong.

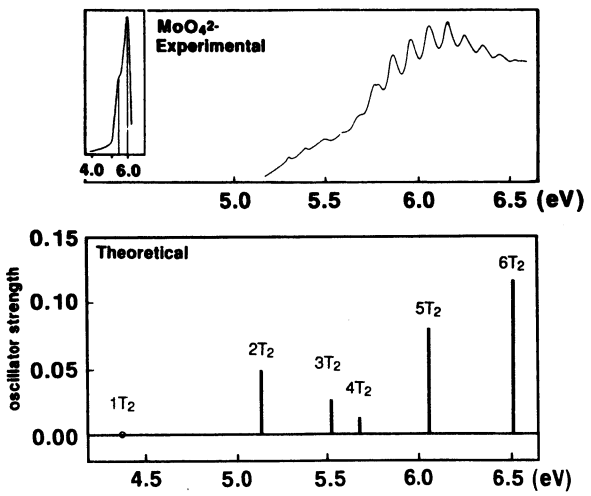

FIG. 4. Experimental and theoretical electronic spectra of MoO_4^{2-}. The open circle O indicates an allowed peak whose strength is very small.

Corresponding to the band observed at 4.30 eV, three dipole-allowed transitions to the $1A_1$, $1E$, and $2E$ states are calculated by the SAC-CI theory at 4.08, 4.10, and 4.13 eV. Their main configurations are $4e(S(p))\rightarrow 5e(M(p))$, $4e(S(p))\rightarrow 5e(M(p))$, and $4e(S(p))\rightarrow 4a_1(M(p))$, respectively. These three states are split from the $1T_2$ state of

TABLE V. Excitation energies of MoO_3S^{2-} in eV.

	SAC-CI		
Expt.[a]	ΔE	f[b]	Main configuration[c]
3.15			
4.30	4.08	0.019	$1A_1(4e\rightarrow 5e)$
	4.10	0.010	$1E(4e\rightarrow 5e)$
	4.13	0.013	$2E(4e\rightarrow 4a_1)$
	4.15		$1A_2(4e\rightarrow 5e,4e\rightarrow 6e)$
	4.41		$2A_2(1a_2\rightarrow 6e,4e\rightarrow 5e,4e\rightarrow 6e)$
	4.41	4.2(−4)[d]	$2A_1(1a_2\rightarrow 6e,4e\rightarrow 6e)$
	4.45		$3A_2(4e\rightarrow 6e,4e\rightarrow 5e)$
	4.75	0.013	$3E(4e\rightarrow 6e,1a_2\rightarrow 6e)$
	4.84	0.077	$3A_1(3e\rightarrow 6e)$
	4.93		$4A_2(1a_2\rightarrow 4a_1)$
	4.94	0.036	$4E(4e\rightarrow 4a_1)$
	5.12	0.001	$5E(1a_2\rightarrow 6e)$
	5.17		$5A_2(3e\rightarrow 6e,2a_1\rightarrow 6e)$
	5.20	2.5(−4)[d]	$6E(3e\rightarrow 6e)$

Average discrepancy 0.20

[a] Reference 5.
[b] Oscillator strenth.
[c] Indicated relative to the HF configuration $(1e)^4(2e)^4(1a_1)^2(2a_1)^2(3e)^4(1a_2)^2(3a_1)^2(4e)^4$.
[d] Characteristic base 10 given in parentheses.

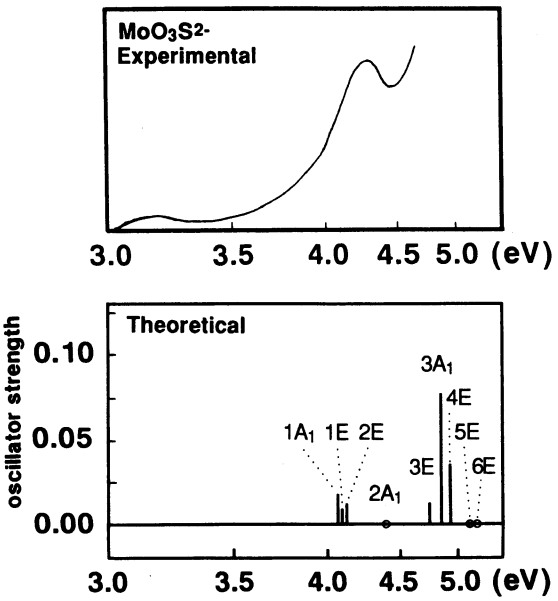

FIG. 5. Experimental and theoretical electronic spectra of MoO_3S^{2-}. The open circle O is an allowed peak whose strength is very small.

MoO_4^{2-}. The theoretical transition energies are smaller than the experimental ones, probably because of the solvent effect.

Beyond 4.30 eV, we expect the next peak at around 4.8–4.9 eV, owing to the $3E$, $3A_1$, and $4E$ states. Table V gives their main configurations. The electron correlation should be important for these states, particularly for the $3E$ state, because the main configuration is unable to be represented by a single configuration.

3. $MoO_2S_2^{2-}$

Figure 7 shows the experimental excitation spectrum of $MoO_2S_2^{2-}$ observed in an aqueous solution[7] together with the present theoretical one. Table VI shows the corresponding numerical values of the experimental and theoretical excitation energies and the main configurations of the excited states. The higher four occupied MOs, $4a_1$, $3b_1$, $2a_2$, and $3b_2$, are the orbitals localized on the two S ligands. The lower three virtual MOs, $5a_1$, $4b_1$, and $4b_2$, consist of the metal p orbitals and related to the $3t_2$ MO of MoO_4^{2-}. The $6a_1$ MO is antibonding between M(d) and S(p) and is related to the $2e$ MO of MoO_4^{2-}.

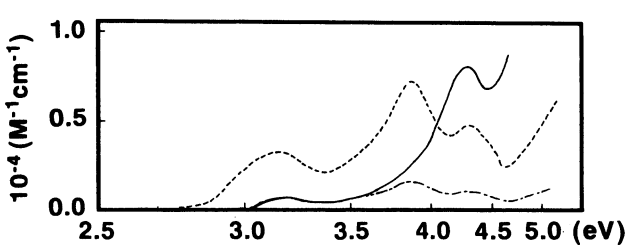

FIG. 6. Electronic spectra of MoO_3S^{2-}, $MoO_2S_2^{2-}$ and scaled $MoO_2S_2^{2-}$. The solid line (——), broken line (– – –), and dashed-dotted line (– · –) correspond to MoO_3S^{2-}, $MoO_2S_2^{2-}$ and scaled $MoO_2S_2^{2-}$, respectively.

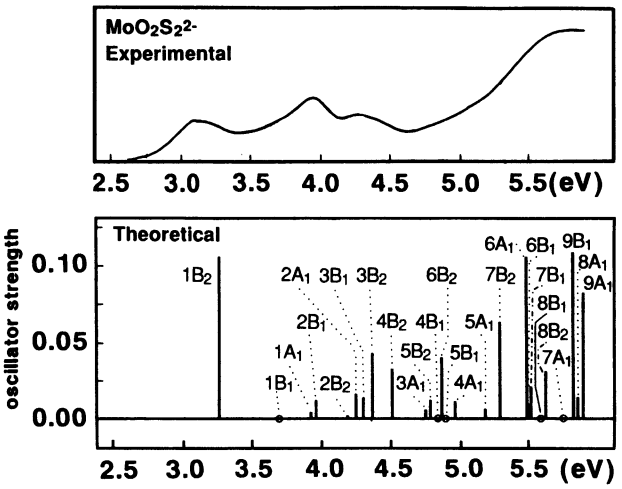

FIG. 7. Experimental and theoretical electronic spectra of $MoO_2S_2^{2-}$. The open circle O is an allowed peak whose strength is very small.

TABLE VI. Excitation energies of $MoO_2S_2^{2-}$ in eV.

Expt.[a]		SAC-CI		
ΔE	f[b]	ΔE	f[b]	Main configuration[c]
		3.34		$1A_2(2a_2\rightarrow 6a_1)$
3.15	0.05	3.36	0.106	$1B_2(3b_2\rightarrow 6a_1,3b_2\rightarrow 5a_1)$
		3.69	0.001	$1B_1(3b_1\rightarrow 6a_1,3b_2\rightarrow 3a_2)$
		3.91	0.005	$1A_1(3b_2\rightarrow 4b_2)$
		3.94	0.013	$2B_1(3b_2\rightarrow 3a_2)$
		4.09		$2A_2(3b_2\rightarrow 4b_1)$
3.89	0.1	4.18	0.003	$2B_2(3b_2\rightarrow 5a_1,3b_1\rightarrow 3a_2)$
		4.24	0.017	$2A_1(2a_2\rightarrow 3a_2)$
		4.29	0.015	$3B_1(2a_2\rightarrow 4b_2)$
		4.36	0.044	$3B_2(2a_2\rightarrow 4b_1)$
4.30	0.04	4.50	0.034	$4B_2(2b_1\rightarrow 3a_2,2a_2\rightarrow 4b_1,3b_1\rightarrow 3a_2)$
		4.56		$3A_2(2a_2\rightarrow 5a_1)$
		4.62		$4A_2(3b_1\rightarrow 4b_2)$
		4.74	0.007	$3A_1(3b_1\rightarrow 4b_1)$
		4.77	0.013	$5B_2(2b_2\rightarrow 6a_1,2b_2\rightarrow 5a_1)$
		4.83	2.9(−4)[d]	$4B_1(2b_1\rightarrow 6a_1)$
		4.85	0.041	$6B_2(2b_2\rightarrow 6a_1)$
		4.88	9.2(−4)[d]	$5B_1(3b_1\rightarrow 5a_1)$
		4.94	0.012	$4A_1(4a_1\rightarrow 6a_1,3b_2\rightarrow 5b_2,4a_1\rightarrow 5a_1)$
		4.99		$5A_2(4a_1\rightarrow 3a_2)$
		5.17	0.007	$5A_1(3b_2\rightarrow 5b_2,3a_1\rightarrow 6a_1,4a_1\rightarrow 6a_1)$
		5.27	0.064	$7B_2(2b_1\rightarrow 3a_2,3b_1\rightarrow 3a_2)$
5.66		5.34		$6A_2(2a_2\rightarrow 7a_1)$
		5.47	0.106	$6A_1(3a_1\rightarrow 6a_1,3b_2\rightarrow 5b_2)$
		5.48	0.010	$6B_1(2a_2\rightarrow 5b_2,2b_1\rightarrow 5a_1,2b_2\rightarrow 3a_2)$
		5.50	0.022	$7B_1(2b_2\rightarrow 3a_2,3b_1\rightarrow 7a_1,2a_2\rightarrow 5b_2)$
		5.57	0.001	$8B_1(4a_1\rightarrow 4b_1,2a_2\rightarrow 5b_2,2b_2\rightarrow 3a_2)$
		5.61	0.032	$8B_2(4a_1\rightarrow 4b_2)$
		5.73	1.7(−4)[d]	$7A_1(4a_1\rightarrow 5a_1)$
		5.78		$7A_2(3b_2\rightarrow 5b_1,2b_1\rightarrow 5b_2,3a_1\rightarrow 3a_2)$
		5.81	0.109	$9B_1(3b_1\rightarrow 7a_1,4a_1\rightarrow 4b_1)$
		5.84	0.015	$8A_1(2b_1\rightarrow 4b_1)$
		5.88	0.083	$9A_1(2b_2\rightarrow 4b_2)$
		5.92		$8A_2(2b_2\rightarrow 4b_1,3b_1\rightarrow 5b_2,2b_1\rightarrow 4b_2)$
		5.93		$9A_2(2b_2\rightarrow 4b_1,3b_1\rightarrow 5b_2,3a_1\rightarrow 3a_2)$

Average discrepancy 0.25

[a] Reference 7.
[b] Oscillator strength.
[c] Indicated relative to the HF configuration $(1a_1)^2(1b_1)^2(1a_2)^2(1b_2)^2(2a_1)^2(2b_1)^2(3a_1)^2(2b_2)^2(4a_1)^2(3b_1)^2(2a_2)^2(3b_2)^2$.
[d] Characteristic base 10 given in parentheses.

The first peak is observed at 3.15 eV. This peak is assigned to the $1B_2$ state $[3b_2(S(p)) \rightarrow 6a_1(M(d) - S(p))]$ calculated at 3.36 eV, and is related to the transition $1t_1 \rightarrow 2e$ in the T_d symmetry. This is in contrast to the lowest observed peaks of MoO_4^{2-} and MoO_3S^{2-} which are attributed to the transition $2t_2 \rightarrow 3t_2$ in the T_d symmetry. This is due to the stabilization of the $2e$ MO by the ligand substitution as seen in Fig. 1. The calculated oscillator strength of this peak is, however, a little larger than the observed one.

The second band is observed at 3.89 eV. As seen in the experimental spectrum shown in Fig. 7, this band gently slopes down in a lower energy side. This fact suggests that several excited states are involved in this absorption band. In this calculation, several states with relatively small intensities are calculated in this energy region. They are $2B_1[3b_2(S(p)) \rightarrow 3a_2(M(d) - O(p) - S(p))]$, $2A_1[2a_2 \times (S(p)) \rightarrow 3a_2(M(d) - O(p) - S(p))]$, $3B_1[2a_2(S(p))] \rightarrow 4b_2(M(p))]$, and $3B_2[2a_2(S(p)) \rightarrow 4b_1(M(p))]$ and some others. Among these the $3B_2$ state has largest intensity and would be assigned as the main peak of the second band, though the energy is about 0.5 eV higher than the experimental band maximum. The oscillator strengths of these peaks sum up to 0.097, which is comparable to the observed intensity. These transitions correspond to the transitions, $1t_1 \rightarrow 3t_2$ and $1t_1 \rightarrow 2e$, in the T_d symmetry. The assignment by the SCCC-MO calculation,[12] $\sigma_1(S3p - Mo4d) \rightarrow E(Mo4d)$, differs from the result of the present study.

The observed band at 4.30 eV is assigned to the $4B_2$ state for its energy and oscillator strength. Table VI shows that this state is mainly constructed by three configurations and that the configuration mixing is large. Consequently, the assignment of this state by the calculations without taking into account of electron correlations is not reliable. The electron correlations are essential for many states listed in Table VI. In the present calculation, there is ca. 0.4 eV between the excitation energies of the second band of MoO_3S^{2-} and the third band of $MoO_2S_2^{2-}$. The relationship (2) stated in the introduction is, however, essentially correct.

In the experimental spectrum of Fig. 7, a very broad and strong band system starts from ca. 4.7 eV and the band maximum is measured at 5.66 eV. Table VI shows that the excited states continuously exist beyond 4.74 eV. The main theoretical peaks are the $6A_1$ and $9B_1$ states calculated at 5.47 and 5.81 eV, respectively. Furthermore, many other excited states have large oscillator strengths and cause a broadness of the band. This is due to the reduction of the symmetry from T_d to C_{2v}. We particularly note the importance of electron correlations for the states composing this broad band system.

The average discrepancy of the theoretical excitation energies from the experimental ones is 0.25 eV.

4. $MoOS_3^{2-}$

Table VII gives the experimental and theoretical excitation energies and oscillator strengths. The experimental spectrum shown in Fig. 8 was observed in an aqueous solution of Cs_2MoOS_3.[8]

The lowest weak peak at 2.67 eV is assigned to the $1E$ state $[1a_2(S(p)) \rightarrow 6e(M(p,d) - S(p))]$ calculated at 2.86 eV. This transition corresponds to the transition $1t_1 \rightarrow 2e$ in the T_d symmetry, as the first peak of $MoO_2S_2^{2-}$. The assignment by the SCCC-MO calculation[12] is the same, but the character of the $6e$ MO is different. It is $M(d)$ in the SCCC-MO calculation,[12] but in the present study it is an antibonding orbital between $M(p,d)$ and $S(p)$. The present results of

TABLE VII. Excitation energies of $MoOS_3^{2-}$ in eV.

Expt.[a]		SAC-CI		
ΔE	f[b]	ΔE	f[b]	Main configuration[c]
2.67		2.86	0.013	$1E(1a_2 \rightarrow 6e, 1a_2 \rightarrow 5e)$
		2.95		$1A_2(4e \rightarrow 6e)$
3.16	0.1	3.31	0.061	$1A_1(4e \rightarrow 7e, 4e \rightarrow 5e)$
		3.33	0.067	$2E(4e \rightarrow 6e, 4e \rightarrow 5e)$
		3.97	0.001	$3E(1a_2 \rightarrow 5e, 1a_2 \rightarrow 6e)$
		4.02		$2A_2(1a_2 \rightarrow 4a_1)$
		4.15	0.012	$4E(3e \rightarrow 6e, 3a_1 \rightarrow 6e)$
3.97	0.09	4.26		$3A_2(3e \rightarrow 6e, 4e \rightarrow 5e)$
		4.29	0.013	$5E(4e \rightarrow 5e, 3a_1 \rightarrow 6e)$
		4.33	0.003	$2A_1(4e \rightarrow 5e)$
		4.40	0.005	$6E(4e \rightarrow 4a_1)$
		4.51		$4A_2(4e \rightarrow 5e, 3e \rightarrow 6e)$
4.77		4.65	0.043	$3A_1(3e \rightarrow 6e, 3e \rightarrow 5e)$
		4.65	0.048	$7E(3e \rightarrow 6e, 4e \rightarrow 5e)$
		4.98		$5A_2(1a_2 \rightarrow 5a_1)$
		5.07	0.006	$8E(1a_2 \rightarrow 7e)$
		5.24	0.002	$9E(2a_1 \rightarrow 6e, 4e \rightarrow 7e)$
		5.31	0.002	$10E(2a_1 \rightarrow 6e, 4e \rightarrow 7e)$
		5.35	0.048	$11E(3a_1 \rightarrow 5e, 4e \rightarrow 5a_1)$
5.10	0.38	5.38		$6A_2(4e \rightarrow 7e)$
		5.47	0.012	$4A_1(3a_1 \rightarrow 4a_1)$
		5.56	0.042	$5A_1(4e \rightarrow 7e, 3a_1 \rightarrow 4a_1)$
		5.60		$7A_2(1a_2 \rightarrow 6a_1)$
		5.63	0.085	$12E(3e \rightarrow 5e, 4e \rightarrow 5a_1)$
		5.69	0.001	$13E(3e \rightarrow 4a_1)$
		5.70		$8A_2(3e \rightarrow 5e)$
		5.81	0.006	$14E(3e \rightarrow 4a_1, 4e \rightarrow 5a_1)$
		5.84	0.080	$6A_1(3e \rightarrow 5e, 3a_1 \rightarrow 4a_1)$

Average discrepancy 0.22

[a] Reference 8.
[b] Oscillator strength.
[c] Indicated relative to the HF configuration $(1a_1)^2(1e)^4(2e)^4(2a_1)^2(3e)^4(3a_1)^2(4e)^4(1a_2)^2$.

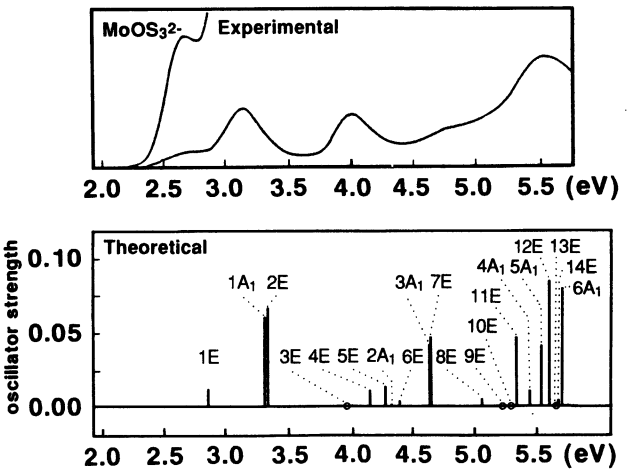

FIG. 8. Experimental and theoretical electronic spectra of $MoOS_3^{2-}$. The open circle O is an allowed peak whose strength is very small.

the excitation energy and the oscillator strength compare well with the experimental values.

In the experimental spectrum, the maximum of the second band is measured at 3.16 eV. This band was assigned to $5e(\pi(\mathrm{S}3p-\mathrm{Mo}4d))\rightarrow 6e(E(\mathrm{Mo}4d))$ in the SCCC-MO calculation.[12] However, we attribute this band to the $1A_1$ state $[4e(\mathrm{S}(p))\rightarrow 7e(\mathrm{M}(d)-\mathrm{O}(p)-\mathrm{S}(p))]$ and the $2E$ state $[4e(\mathrm{S}(p))\rightarrow 6e(\mathrm{M}(p,d)-\mathrm{S}(p))]$ calculated at 3.31 and 3.33 eV, respectively. The energy difference of these states is only 0.02 eV so that the second band looks like a single peak in the experimental spectrum. The calculated oscillator strength is a bit larger than the experimental one. In the Introduction, we have mentioned that the relation (1) is supposed by the experimentalists. However, in Sec. III B 2, we have shown that the first band at 3.15 eV in the spectrum of MoO_3S^{2-} should be attributed to $MoO_2S_2^{2-}$. Consequently, we have to replace the relation (1) of the introduction by the following one,

$$\nu_1(\mathrm{MoO_2S_2^{2-}})\approx\nu_2(\mathrm{MoOS_3^{2-}}), \qquad (1')$$

which is confirmed by the present calculation. Since the transition in (1') are from the orbitals mainly localized on S atoms to the antibonding orbitals between $\mathrm{M}(d)$ and $\mathrm{S}(p)$, these excitation energies are almost same.

The third band at 3.97 eV is also broad and, in particular, has a tail in the higher energy side. The calculation shows there are five allowed states, $3E$, $4E$, $5E$, $2A_1$, and $6E$, in this energy region, though all the states have only small oscillator strengths. From the oscillator strength, we consider that the $4E$ and $5E$ states form mainly this band and the tail in a higher energy region is attributed to the $2A_1$ and $6E$ states. Five transitions in this band system correspond to the transitions, $1t_1\rightarrow 3t_2$ and $1t_1\rightarrow 2e$, in the T_d symmetry.

In the experimental spectrum, a shoulder peak is observed at 4.77 eV. This shoulder is assigned to the $3A_1$ and $7E$ states, whose main configurations both are $3e(\mathrm{O}(p)+\mathrm{S}(p))\rightarrow 6e(\mathrm{M}(p,d)-\mathrm{S}(p))$, though the calculated oscillator strengths are somewhat large. Furthermore, a very broad and intense band is observed around 5.47 eV. The present calculation shows this band system chiefly consists of the $11E$, $5A_1$, and $12E$ states. The broadness is understood since many other states with small intensities exist in this region as seen from Table VII.

The average discrepancy between the experimental and theoretical excitation energies is 0.22 eV. In Fig.8, the theoretical spectrum reproduces the experimental one very well in whole of the energy region.

5. MoS_4^{2-} and $MoSe_4^{2-}$

Tables VIII and IX summarize the theoretical results of the present and previous studies[11–14] and the experimental

TABLE VIII. Excitation energies of MoS_4^{2-} in eV.

Expt.[a]		SAC-CI			SCCC[b]		$X\alpha$[c]		$X\alpha$[d]		LDT[e]	
ΔE	f[f]	ΔE	f[f]	Main configuration[g]	ΔE	Assign.	ΔE	Assign.	ΔE	Assign.	ΔE	Assign.
									2.0	$1t_1\rightarrow 2e$		
2.37		2.58		$1T_1(1t_1\rightarrow 2e)$								
2.65	0.1	3.03	0.157	$1T_2(1t_1\rightarrow 2e)$	3.17	$1t_1\rightarrow 2e$	1.87	$1t_1\rightarrow 2e$	2.7	$2t_2\rightarrow 2e$	2.50	$1t_1\rightarrow 2e$
							2.52	$2t_2\rightarrow 2e$				
3.22		3.69		$2T_1(1t_1\rightarrow 3t_2,1t_1\rightarrow 2e)$								
		3.75		$1E(1t_1\rightarrow 3t_2)$								
		3.83	0.037	$2T_2(1t_1\rightarrow 3t_2)$			3.53	$1t_1\rightarrow 3t_2$	3.4	$1t_1\rightarrow 3t_2$	3.50	$2t_2\rightarrow 2e$
3.91	0.2	3.88		$1A_2(1t_1\rightarrow 3t_2)$			4.19	$2t_2\rightarrow 3t_2$			3.89	$1t_1\rightarrow 3t_2$
		4.19		$3T_1(2t_2\rightarrow 2e,1t_1\rightarrow 3t_2)$								
		4.34	0.095	$3T_2(2t_2\rightarrow 2e)$								
4.62		5.07		$4T_1(1t_1\rightarrow 2a_1,2t_2\rightarrow 3t_2)$								
		5.13		$2E(1a_1\rightarrow 2e)$								
		5.16		$3E(1t_1\rightarrow 4t_2,1t_1\rightarrow 3t_2)$								
		5.18		$2A_2(1t_1\rightarrow 4t_2,1t_1\rightarrow 3t_2)$								
		5.20	4.0(−4)[h]	$4T_2(1t_1\rightarrow 4t_2,2t_2\rightarrow 3t_2)$			3.94	$1t_2\rightarrow 2e$	5.5	$1e\rightarrow 3t_2$	4.90	$2t_2\rightarrow 3t_2$
		5.25		$5T_1(1t_1\rightarrow 4t_2,2t_2\rightarrow 3t_2)$			4.77	$1a_1\rightarrow 3t_2$				
5.12	0.32	5.29		$1A_1(2t_2\rightarrow 3t_2)$								
		5.34		$4E(2t_2\rightarrow 3t_2)$								
		5.48		$6T_1(1t_1\rightarrow 2a_1)$								
		5.65	0.264	$5T_2(2t_2\rightarrow 3t_2,1t_1\rightarrow 4t_2)$								
		5.96		$7T_1(1t_2\rightarrow 2e)$								
		6.06		$5E(1e\rightarrow 2e)$								
5.99		6.31	0.250	$6T_2(1t_2\rightarrow 2e)$								

Average discrepancy 0.32

[a] Reference 4.
[b] Reference 11.
[c] Reference 14.
[d] Reference 15.
[e] Reference 16.
[f] Oscillator strength.
[g] Indicated relative to the HF configuration $(1t_2)^6(1e)^4(1a_1)^2(2t_2)^6(1t_1)^6$.
[h] Characteristic base 10 given in parenthesis.

TABLE IX. Excitation energies of $MoSe_4^{2-}$ in eV.

	SAC-CI			SCCC[b]		$X\alpha$[c]	
Expt.[a]	ΔE	f[d]	Main configuration[e]	ΔE	Assign.	ΔE	Assign.
2.0	2.03		$1T_1(1t_1\rightarrow 2e)$				
2.23	2.44	0.157	$1T_2(1t_1\rightarrow 2e)$	2.07	$1t_1\rightarrow 2e$	1.55	$1t_1\rightarrow 2e$
						2.29	$2t_2\rightarrow 2e$
2.75	3.18		$2T_1(1t_1\rightarrow 3t_2, 2t_2\rightarrow 2e)$				
	3.21		$1E(1t_1\rightarrow 3t_2)$				
	3.33		$1A_2(1t_1\rightarrow 3t_2)$				
3.45	3.37	0.057	$2T_2(1t_1\rightarrow 3t_2)$			3.21	$1t_1\rightarrow 3t_2$
	3.75		$3T_1(2t_2\rightarrow 2e)$			3.96	$2t_2\rightarrow 3t_2$
	3.84	0.124	$3T_2(2t_2\rightarrow 2e)$				
4.00	4.70		$4T_1(2t_2\rightarrow 3t_2)$				
	4.75		$2E(1a_1\rightarrow 2e, 2t_2\rightarrow 3t_2)$				
	4.80		$1A_1(2t_2\rightarrow 3t_2)$				
4.61	4.82	0.019	$4T_2(1t_1\rightarrow 4t_2, 2t_2\rightarrow 3t_2)$			3.66	$1t_2\rightarrow 2e$
	4.86		$3E(1t_1\rightarrow 4t_2)$			4.65	$1t_1\rightarrow 3t_2$
	4.87		$2A_1(1a_1\rightarrow 2e, 1e\rightarrow 2e)$				
	4.90		$2A_2(1t_1\rightarrow 4t_2, 1t_2\rightarrow 3t_2)$				
	4.91		$5T_1(1t_1\rightarrow 4t_2)$				
	5.20		$3A_2(1e\rightarrow 2e)$				
	5.22		$6T_1(1t_2\rightarrow 3t_2, 1t_2\rightarrow 2e, 1t_1\rightarrow 2a_1)$				
	5.29	0.298	$5T_2(2t_2\rightarrow 3t_2, 1t_1\rightarrow 4t_2, 1t_2\rightarrow 2e)$				
	5.60	0.522	$6T_2(1t_2\rightarrow 2e)$				

Average discrepancy 0.32

[a] Reference 4.
[b] Reference 11.
[c] Reference 14.
[d] Oscillator strength.
[e] Indicated relative to the HF configuration $(1t_2)^6(1e)^4(1a_1)^2(2t_2)^6(1t_1)^6$.

data[4] for MoS_4^{2-} and $MoSe_4^{2-}$, respectively. The experimental and theoretical electronic spectra of MoS_4^{2-} and $MoSe_4^{2-}$ are shown in Figs. 9 and 10, respectively. The experimental and theoretical spectra of MoS_4^{2-} and $MoSe_4^{2-}$ are very similar to each other, though the peaks of $MoSe_4^{2-}$ are shifted by about 0.45 eV toward lower energy in comparison with those of MoS_4^{2-}. However, the spectra of MoS_4^{2-} and $MoSe_4^{2-}$ are quite different from that of MoO_4^{2-}. This similarity and difference are caused by those in their electronic structures and M–L bond strengths among MoO_4^{2-}, MoS_4^{2-}, and $MoSe_4^{2-}$.

As seen in the experimental spectra of Figs. 9 and 10, there is a very weak peak below the first strong peak. This peak has been considered as being due to the spin forbidden or dipole forbidden transition.[3] The present calculation indicates that this peak is assigned to the $1T_1$ state $[1t_1(\mathrm{L}(p))\rightarrow 2e(\mathrm{M}(d)-\mathrm{L}(p))]$ for both complexes. This is a dipole forbidden transition. This assignment is, however, not decisive, since we did not calculate triplet excited states in this study.

The lowest allowed peak is assigned to the $1T_2$ state $[1t_1(\mathrm{L}(p))\rightarrow 2e(\mathrm{M}(d)-\mathrm{L}(p))]$ in both complexes. This transition accompanies an electron transfer from ligands to metal. The relation (4) noted in the Introduction is considered to be valid. The calculated excitation energies and oscillator strengths are a bit larger than the experimental values. On the other hand, the lowest excitation energies calculated by the $X\alpha$ methods[14,15] are smaller by about 0.7 eV than the experimental values for both complexes. Our assignment is the same as most of the previous studies.[4,11,12,14]

There are weak peaks at 3.22 and 4.62 eV in MoS_4^{2-} and

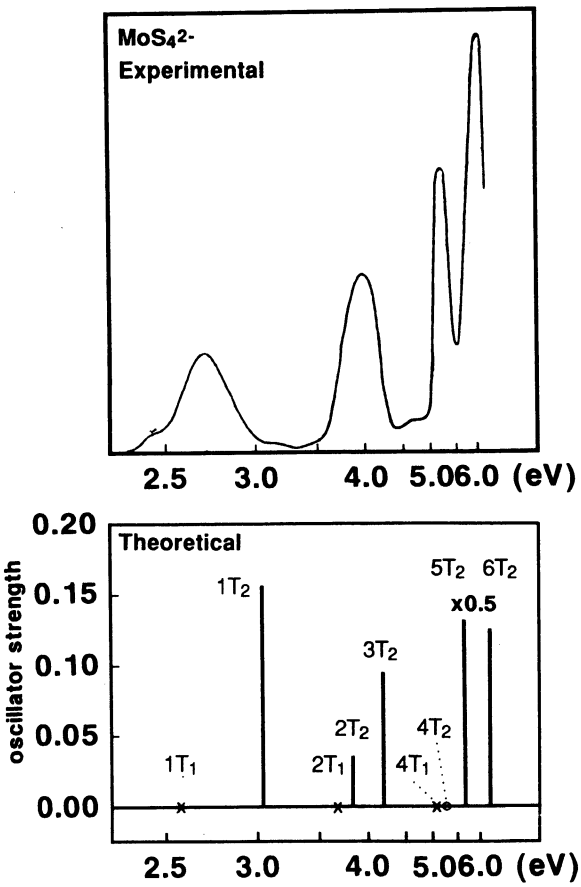

FIG. 9. Experimental and theoretical electronic spectra of MoS_4^{2-}. The open circle O is an allowed peak whose strength is very small and × is a dipole forbidden peak.

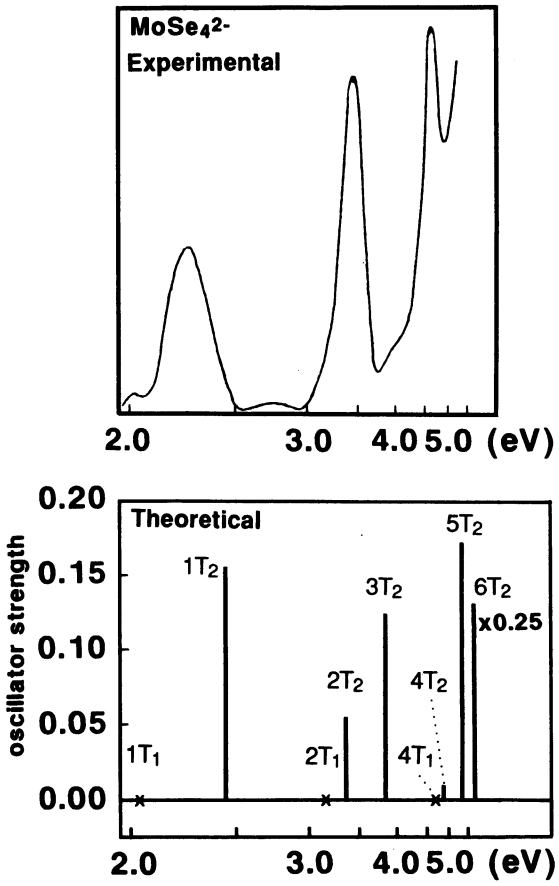

FIG. 10. Experimental and theoretical electronic spectra of $MoSe_4^{2-}$. The cross $\times$ is a dipole forbidden peak.

at 2.75 and 4.00 eV in $MoSe_4^{2-}$, respectively. We assign the lower peak to the $2T_1$ state and the higher one to the $4T_1$ state in both complexes for an energetic reason. These transitions may borrow an intensity from other allowed transitions through a vibronic coupling.

In the $X\alpha$ calculation on MnO_4^{2-},[13] the amount of charge transfer in the so-called "charge transfer" excitations is actually very small. Table X gives the population analyses for the ground and $1T_2$ states of MoO_4^{2-}, MoS_4^{2-}, and $MoSe_4^{2-}$. The present calculation shows that 0.765, 0.160, and 0.184 electrons transfer from L to M in MoO_4^{2-}, MoS_4^{2-}, and $MoSe_4^{2-}$, respectively. The amount of the transferred electron in MoS_4^{2-} is nearly equal to that in $MoSe_4^{2-}$, but the difference of those from that in MoO_4^{2-} is very large.

TABLE X. Atomic net charges of the ground and $1T_2$ states of MoO_4^{2-}, MoS_4^{2-}, and $MoSe_4^{2-}$.

	MoO_4^{2-}		MoS_4^{2-}		$MoSe_4^{2-}$	
State	Mo	O	Mo	S	Mo	Se
Ground	+1.294	−0.823	−0.200	−0.450	−0.259	−0.435
$1T_2$	+0.529	−0.595	−0.360	−0.410	−0.443	−0.389

This is understood since in MoS_4^{2-} and $MoSe_4^{2-}$, the transitions are $L(p) \rightarrow (M(d) - L(p))$, while that in MoO_4^{2-} is $L(p) \rightarrow M(p)$.

The ionicities of the M–L bonds in the ground states of MoS_4^{2-} and $MoSe_4^{2-}$ are small, in contrast to that of MoO_4^{2-}. Therefore, the stabilization of MoS_4^{2-} and $MoSe_4^{2-}$ in a polar solvent is expected to be smaller than that of MoO_4^{2-}. As estimated from the Mulliken atomic net charges given in Table X, the solvation energy for the ground state of MoO_4^{2-} should be larger than that for the $1T_2$ excited state. This is the type I case of Fig. 3 and the excitation energy in a polar solvent should be larger than in vacuum, i.e., $\Delta E^{\mathrm{I}}_{\mathrm{SOL}} > \Delta E^{\mathrm{I}}_{\mathrm{VAC}}$. On the other hand, for MoS_4^{2-} and $MoSe_4^{2-}$ the solvation energies in the ground states should be comparable to that in the excited states, so that the excitation energy is not much affected by a polar solvent. This is type II of Fig. 3.

The asymmetry of the second peaks of MoS_4^{2-} and $MoSe_4^{2-}$, shown in Figs. 9 and 10, suggests an existence of one or more states in the lower energy envelope. In the present calculation, the $2T_2[1t_1(L(p)) \rightarrow 3t_2(M(d))]$ and $3T_2[2t_2(L(p)) \rightarrow 2e(M(d) - L(p))]$ states are calculated for both complexes below and above the experimental band maximum of the second peak. The intensity of the $3T_2$ state is larger than that of the $2T_2$ state. This result explains the shape of the observed spectra. In the previous works, this second band is attributed to the transitions $1t_1 \rightarrow 3t_2$ and $2t_2 \rightarrow 3t_2$,[14] $1t_1 \rightarrow 3t_2$,[15] and $2t_2 \rightarrow 2e$ and $1t_1 \rightarrow 3t_2$.[16] Though the conclusion of the local density calculation[16] is similar to the present one, their ordering of the excited states is different. We believe that the present assignment is correct, since the ordering of these two excited states in MoS_4^{2-} and $MoSe_4^{2-}$ corresponds well with that of the second and third bands in $MoO_2S_2^{2-}$ and $MoOS_3^{2-}$. Thus, the present calculation shows that the relationship (3) noted in the introduction is correct.

A similar situation seems to exist in the third band: it consists of the two allowed $4T_2$ and $5T_2$ states. The sum of the oscillator strengths compare fairly to experiment, though the excitation energies are about 0.5 eV higher. Tables VIII and IX show that the configuration mixing of the transitions $1t_1 \rightarrow 4t_2$ and $2t_2 \rightarrow 3t_2$ is large in these two states. Therefore, the assignments due to the theories without taking account of the configuration mixing, the SCCC-MO calculations,[11] the $X\alpha$ methods,[14,15] and the local density calculations[16] may not be reliable.

The fourth band of MoS_4^{2-} is assigned to the $6T_2$ state $[1t_2(M(d) + L(p)) \rightarrow 2e(M(d) - L(p))]$. Though the fourth band is not observed in $MoSe_4^{2-}$, the $6T_2$ state of $MoSe_4^{2-}$ is the same as that of MoS_4^{2-}. These transitions are remarkable, since all the allowed transitions of the six complexes studied in this paper, except for these transitions, are the electron transferred excitations from ligands like $L \rightarrow M$ and $L \rightarrow (M - L)$.

The average discrepancies of the calculated excitation energies from the experimental ones are 0.32 eV for both MoS_4^{2-} and $MoSe_4^{2-}$. The theoretical spectra in Figs. 9 and 10 show a good correspondence with the experimental ones.

The splitting parameters Δ of MoS_4^{2-} and $MoSe_4^{2-}$ in

the ligand field theory are calculated as 1.44 and 1.38 eV, respectively, in comparison with the experimental values of 1.25 and 1.22 eV (Ref. 4), respectively.

IV. CONCLUSION

Ab initio calculations based on the SAC and SAC-CI theories are reported for the singlet excited states of the six molybdenum complexes, $MoO_{4-n}S_n^{2-}$ $(n=0\sim4)$ and $MoSe_4^{2-}$. In the ground state, the M–L bonds of MoO_4^{2-} are stronger and more ionic than those of MoS_4^{2-} and $MoSe_4^{2-}$. Thus the electronic spectrum of MoO_4^{2-} are much different from those of MoS_4^{2-} and $MoSe_4^{2-}$.

For all complexes, the theoretical electronic spectra reproduce well the experimental spectra and the average discrepancies between the experimental and theoretical excitation energies are within 0.32 eV. We have given many new assignments which differ from the previous ones. All of the observed peaks except for the peak of MoS_4^{2-} at 5.99 eV $(6T_2)$ are due to the electron transfer excitations from L to M or L to (M − L). As the number of the soft ligands (S and Se) increases, the excitation energies of L→(M − L) decrease since the M–L bonds become weaker.

The present study shows that in MoO_3S^{2-}, $MoO_2S_2^{2-}$, and $MoOS_3^{2-}$, the observed bands consist of many dipole allowed peaks because of the splitting of the excited states due to the symmetry lowering from T_d to C_{3v} and C_{2v}.

The relationships (2)∼(4) summarized in the Introduction are confirmed to be essentially correct except for the first equality in the relationship (1). It should be improved as the relationship (1′) given in the preceding section since the lowest peak in the spectrum of MoO_3S^{2-} should be attributed to $MoO_2S_2^{2-}$. The reason of the relationships (1′), (2)∼(4) lies in the similarity of the corresponding excited states.

ACKNOWLEDGMENTS

The calculations have been carried out with the HITAC M680H and S820/80 computers at the Institute for Molecular Science. This study has partially been supported by the Grant-in-Aids for Scientific Research from the Ministry of Education, Science and Culture and by the Kurata Foundation.

[1]H. Nakatsuji and S. Saito, Int. J. Quantum Chem. (in press).
[2]S. Foster, S. Felps, L. W. Johnson, D. B. Larson, and S. P. McGlynn, J. Am. Chem. Soc. **95**, 6578 (1973).
[3]R. Borromei, G. Ingletto, and L. Di Sipio, Chem. Phys. Lett. **92**, 288 (1982).
[4]A. Müller and E. Diemann, Chem. Phys. Lett. **9**, 369 (1971).
[5]A. Müller, E. Diemann, A. C. Ranade, and P. J. Aymonino, Z. Naturforsch. **24b**, 1247 (1969).
[6]M. A. Harmer and A. G. Sykes, Inorg. Chem. **19**, 2881 (1980).
[7]A. Müller, B. Krebs, W. Rittner, and M. Stockburger, Ber. Bunsenges. Phys. Chem. **71**, 182 (1967).
[8]E. Diemann and A. Müller, Spectrochim. Acta **A26**, 215 (1970).
[9]R. H. Petit, B. Briat, A. Müller, and E. Diemann, Chem. Phys. Lett. **20**, 540 (1973); Mol. Phys. **27**, 1373 (1974).
[10]P. J. Aymonino, A. C. Ranade, and A. Müller, Z. Anorg. Allg. Chem. **371**, 295 (1969).
[11]R. Kebabcioglu and A. Müller, Chem. Phys. Lett. **8**, 59 (1971).
[12]R. Jostes, A. Müller, and E. Diemann, J. Mol. Struct. (Theochem.) **137**, 311 (1986).
[13]T. Ziegler, A. Rauk, and E. J. Baerends, Chem. Phys. **16**, 209 (1976).
[14]D. E. Onopko and S. A. Titov, Opt. Spectrosc. (Engl. Transl.) **47**, 185 (1979).
[15]F. W. Kutzler, C. R. Natoli, D. K. Misemer, S. Doniach, and K. O. Hodgson, J. Chem. Phys. **73**, 3274 (1980).
[16]J. Bernholc and E. I. Stiefel, Inorg. Chem. **24**, 1323 (1985).
[17]O. Lutz, A. Nolle, and P. Kroneck, Z. Naturforsch. **32a**, 505 (1977); P. Kroneck, O. Lutz, and A. Nolle, *ibid.* **35a**, 226 (1980); S. F. Gheller, P. A. Gazzana, A. F. Masters, R. T. C. Brownlee, M. J. O'Connor, A. G. Wedd, J. R. Rodgers, and M. R. Snow, Inorg. Chimica Acta **54**, L131 (1981); S. F. Gheller, T. W. Hambley, J. R. Rodgers, R. T. C. Brownlee, M. J. O'Connor, M. R. Snow, and A. G. Wedd, Inorg. Chem. **23**, 2519 (1984).
[18]H. Nakatsuji and M. Sugimoto, Inorg. Chem. **29**, 1221 (1990).
[19]H. Nakatsuji, M. Sugimoto, and S. Saito, Inorg. Chem. (in press).
[20]A. Kalman, J. Chem. Soc. A 1857 (1971).
[21]F. W. Kutzler, R. A. Scott, J. M. Berg, K. O. Hodgson, S. Doniach, S. P. Cramer, and C. H. Chang, J. Am. Chem. Soc. **103**, 6083 (1981).
[22]B. Krebs, A. Müller, and E. Kindler, Z. Naturforsch. **25b**, 222 (1970).
[23]M. G. Kanatzidis and D. Coucouvanis, Acta Crystallogr. Sect. C. Cryst. Struct. Commun. **C39**, 835 (1983).
[24]A. Müller, E. Diemann, and U. Heidborn, Z. Anorg. Allg. Chem. **376**, 125 (1970).
[25]P. J. Hay, and W.R. Wadt, J. Chem. Phys. **82**, 270 (1985).
[26]S. Huzinaga, *Gaussian Basis Sets for Molecular Calculation* (Elsevier, Amsterdam, 1984).
[27]W. R. Wadt and P. J. Hay, J. Chem. Phys. **82**, 284 (1985).
[28]B. R. Brooks, P. Saxe, W. D. Laidig, and M. Dupuis, Program System GAMESS; Program Library No. 481, Computer Center of the Institute for Molecular Science, 1981.
[29]H. Nakatsuji and K. Hirao, J. Chem. Phys. **68**, 2053 (1978).
[30]H. Nakatsuji, Chem. Phys. Lett. **59**, 362 (1978).
[31]H. Nakatsuji, Program System for SAC and SAC-CI Calculations, Program Library No. 146 (Y4/SAC), Data Processing Center of Kyoto University (1985). Program Library SAC85, No. 1396, Computer of the Institute for Molecular Science (1981).
[32]H. Nakatsuji, Chem. Phys. **75**, 425 (1983).
[33]E. Diemann and A. Müller, Coord. Chem. Rev. **10**, 79 (1973).
[34]L. Pauling, *The Nature of Chemical Bond*, 3rd Ed. (Cornell University Press, Ithaca, 1960).
[35]A. Müller, E. Diemann, F. Neumann, and R. Menge, Chem. Phys. Lett. **16**, 521 (1972).
[36]A. Müller, H. Dornfeld, H. Schulze, and R. C. Sharma, Z. Anorg. Allg. Chem. **468**, 193 (1980).